ISSN: 0067-2904

Elastic electron scattering from 11Li and 12Be exotic nuclei in the framework of the binary cluster model

Adel K. Hamoudi , Ahmed N. Abdullah
Department of Physics, College of Science, University of Baghdad, Baghdad, Iraq

Abstract

The ground state densities of unstable neutron-rich 11Li and 12Be exotic nuclei are studied in the framework of the binary cluster model (BCM). The internal densities of the clusters are described by the single particle harmonic oscillator wave functions. The long tail performance is clearly noticed in the calculated neutron and matter density distributions of these nuclei. The structures of the two valence neutrons in 11Li and 12Be are found to be mixed configurations with dominant (1p1/2)2. Elastic electron scattering proton form factors for 11Li and 12Be are studied using the plane wave Born approximation (PWBA). It is found that the major difference between the calculated form factors of unstable nuclei [11Li, 12Be] and those of stable nuclei [7Li, 9Be] is the difference in the center of mass correction which depends on the mass number and the size parameter . The reaction cross sections for 11Li and 12Be are studied by means of the Glauber model with an optical limit approximation using the ground state densities of the projectile and target, where these densities are described by single Gaussian functions. The calculated reaction cross sections of 11Li and 12Be at high energy are in good agreement with experimental data. The analysis of the present study supports the halo structure of these nuclei.

Keywords: neutron-rich exotic nuclei; elastic electron scattering form factor; density distributions; root mean square radii of halo nuclei

الاستطارة الالكترونية المرنة من النوى الغريبة ^{11}Li و ^{12}Be باستخدام الانموذج العنقودي الثنائي

عادل خلف حمود ، أحمد نجم عبدالله

قسم الفيزياء ، كلية العلوم، جامعة بغداد، بغداد، العراق

الخلاصة

تم حساب توزيعات الكثافة للنوى الغريبة غير المستقرة والغنية بالنيوترونات ^{11}Li و ^{12}Be باستخدام الانموذج العنقودي الثنائي (BCM). تم وصف الكثافة الداخلية للعنقودين باستخدام الدوال الموجية للجسيمة المفردة لجهد المتذبذب التوافقي. الامتداد الطويل ظهر بوضوح في توزيعات الكثافة النيوترونية والكتلية لهذه النوى.[i]

اوضحت هذه الدراسة بان النيوكليونات الفعالة للنوى ^{11}Li و ^{12}Be تتركب من حالات ممتزجة وبهيمنة التشكيل $(1p_{1/2})^2$. لقد تم تحليل نتائج عوامل التشكل المرنة لبروتونات هذه النوى بواسطة تقريب بورن للموجة المستوية.

*Email: Ahmednajim1979@yahoo.com

وجد ان الاختلاف بين عوامل التشكل للنوى الغريبة [^{11}Li, ^{12}Be] ونظيرتها المستقرة [^{7}Li, ^{9}Be] يعود الى التباين في عامل تصحيح مركز الكتلة والذي يعتمد على العدد الكتلي وثابت المتذبذب التوافقي (α).
تمت دراسة المقاطع العرضية للتفاعل لهذه النوى عند الطاقات العالية باستخدام نموذج غلوبر باستخدام توزيع الكثافة للحالة الارضية للنواة القذيفة والنواة الهدف، حيث ان هذه الكثافات توصف بواسطة دوال جاوس للجسيمة المنفردة.
وجد بان حسابات المقاطع العرضية للتفاعل لهذه النوى تتفق بشكل جيد مع القيم العملية.

1. Introduction

Nuclear size and density distributions are the basic quantities to describe nuclear properties [1]. The charge densities can give us much detailed information on the internal structure of nuclei since they are directly related to the wave functions of protons, which are important keys for many calculations in nuclear physics. Electron–nucleus scattering is known to be one of the powerful tools for investigating nuclear charge density distributions. Charge density distributions for stable nuclei have been well studied with this method [2, 3].

The development of radioactive isotope beam techniques has opened a new field for the study of unstable nuclei far from the stability line [4]. As a result, our knowledge of nuclear physics has also been extended from stable nuclei to unstable ones. Experiments with radioactive isotope beams have already shown that the properties of unstable nuclei are quite different from those of stable ones [5]. Therefore, it is very interesting to investigate the properties of unstable nuclei theoretically with reliable theories and models.

Halo nuclei, which have an extraordinary ratio of protons and neutrons (the proton–rich or neutron–rich) and are so short lived, cannot be used as targets at rest due to their unstable properties. Instead, direct reaction with radioactive isotopes beam can be done in inverse kinematics, where the role of beam and target are interchanged [6]. The charge and matter distributions of these nuclei are tested in analysis of differential and total reaction cross sections of proton scattering on halo nuclei by using different phenomenological and theoretical methods. Concerning the charge distributions of nuclei, it is known that their most accurate determination can be obtained from electron-nucleus scattering. For the case of halo nuclei the corresponding charge densities are planned to be obtained by colliding electrons with those nuclei [6].

Hamoudi *et al*. [7] have studied the ground state densities of unstable proton-rich ^{9}C, ^{12}N and ^{23}Al exotic nuclei in the framework of the two-frequency shell model (TFSM) and the binary cluster model (BCM). In BCM, the internal densities of the clusters are described by single particle Gaussian wave functions. They found that the calculated results are in very good agreement with experimental data.

One of the widely used models for analyzing the interaction and the reaction cross sections of nucleus-nucleus scattering is the Glauber model. The Glauber theory has had considerable success in describing high energy hadron-nucleus scattering [8] and it was natural to extend the Glauber theory to nucleus-nucleus scattering.

In the present study, we analyze the ground state densities, elastic electron scattering proton form factors and reaction cross sections of unstable neutron-rich ^{11}Li and ^{12}Be exotic nuclei. The structure of the two valence neutrons in ^{11}Li and ^{12}Be is investigated and found to be a mixed configurations with dominant $(1p_{1/2})^2$. Elastic electron scattering proton form factors for ^{11}Li [^{12}Be] is studied through combining the proton density distribution with the PWBA. The difference between the calculated form factors of unstable exotic nucleus ^{11}Li [^{12}Be] and that of stable nucleus ^{7}Li [^{9}Be] is analyzed and attributed to the difference in the center of mass correction which depends on the mass number and the size parameter α (which is assumed in this case as the average of α_c and α_v). The reaction cross sections for ^{11}Li [^{12}Be] is examined by means of the Glauber model with an optical limit approximation using the ground state densities of the projectile and target. The calculated reaction cross sections at high energies are in good agreement with experimental data. The analysis of the present study suggests a halo structure for these exotic nuclei.

2. Theory

The one-body operator of the longitudinal transition density for point protons (with isospin $t_z = 1/2$) or neutrons ($t_z = -1/2$) is given by [9]

$$\hat{\rho}^{L}_{\Delta J,t_z} = \sum_{k=1}^{A} e(t_z) \frac{\delta(r - r_k)}{r_k^2} Y_{\Delta J, M_{\Delta J}}(\Omega_{r_k}), \tag{1}$$

with

$$e(t_z) = \frac{1 + 2t_z(k)}{2}.$$

In Eq. (1), the superscript (L) in the operator $\hat{\rho}^{L}_{\Delta J,t_z}$ stands for a longitudinal operator, $Y_{\Delta J, M_{\Delta J}}(\Omega_{r_k})$ and $\delta(\vec{r} - \vec{r}_k)$ are the spherical harmonic and Dirac delta functions, respectively. The multipolarity ΔJ of the transition is restricted by the following angular momentum and parity selection rules:

$\left| J_i \_ J_f \right| \le \Delta J \le J_i + J_f$

and

$\pi_i \pi_f = (-1)^{\Delta J}$ (for Coulomb transitions).

The reduced matrix element of Eq. (1) is expressed as [9]

$$\left\langle J_f \left\| \hat{\rho}^{L}_{\Delta J,t_z}(\vec{r}) \right\| J_i \right\rangle = \frac{1}{\sqrt{4\pi(2J_i + 1)}} \sum_{ab} OBDM(J_f, J_i, \Delta J, a, b, t_z) \left\langle j_a \left\| Y_{\Delta J} \right\| j_b \right\rangle R_{n_a l_a}(r) R_{n_b l_b}(r), \tag{2}$$

where a and b label single-particle states for the considered shell model space, i.e. $|a\rangle = |n_a l_a\rangle |j_a m_a\rangle$ and $|b\rangle = |n_b l_b\rangle |j_b m_b\rangle$, the states $|J_i\rangle$ and $|J_f\rangle$ are characterized by the model space wave functions, $R_{n_p l_p}(r)$ is the radial part of the harmonic oscillator wave function, $\left\langle j_a \left\| Y_{\Delta J} \right\| j_b \right\rangle$ is the reduced matrix element of the spherical harmonic, $OBDM(J_f, J_i, \Delta J, a, b, t_z)$ is the proton ($t_z = 1/2$) or neutron ($t_z = -1/2$) one body density matrix element given by second quantization as [9]

$$OBDM(J_f, J_i, \Delta J, a, b, t_z) = \frac{\left\langle J_f \left\| \left[a^{+}_{a,t_z} \otimes \tilde{a}_{b,t_z} \right]^{\Delta J} \right\| J_i \right\rangle}{\sqrt{2\Delta J + 1}}. \tag{3}$$

As the model space wave functions have good isospin, it is appropriate to evaluate the *OBDM* elements by means of isospin-reduced matrix elements. The relation between these triply reduced *OBDM* and the proton or neutron *OBDM* of Eq. (2) is given by [9]

$$\begin{aligned} OBDM(t_z) = {} & (-1)^{T_f - T_z} \sqrt{2} \begin{pmatrix} T_f & 0 & T_i \\ -T_z & 0 & T_z \end{pmatrix} OBDM(\Delta T = 0)/2 \\ & + 2t_z (-1)^{T_f - T_z} \sqrt{6} \begin{pmatrix} T_f & 1 & T_i \\ -T_z & 0 & T_z \end{pmatrix} OBDM(\Delta T = 1)/2 \end{aligned} \tag{4}$$

where the triply reduced $OBDM(\Delta T)$ elements are given in terms of second quantization as

$$OBDM(i, f, \Delta J, \alpha, \beta, \Delta T) = \frac{\left\langle \Gamma_f \left\| \left[a^{+}_{\alpha} \otimes \tilde{a}_{\beta} \right]^{\Delta J, \Delta T} \right\| \Gamma_i \right\rangle}{\sqrt{2\Delta J + 1}\sqrt{2\Delta T + 1}} \tag{5}$$

Here, Greek symbols are utilized to indicate quantum numbers in coordinate space and isospace (i.e., $\alpha \equiv at_a$, $\beta \equiv bt_b$, $\Gamma_i \equiv J_i T_i$ and $\Gamma_f \equiv J_f T_f$).

The $OBDM(\Delta T)$ elements contain all of the information about transitions of given multipolarities which are embedded in the model space wave functions. To obtain these *OBDM* elements, we perform shell model calculations by OXBASH code [10] using realistic effective interactions.

For the ground state density distribution, we have $n_a = n_b$, $l_a = l_b$, $j_a = j_b$, $J_i = J_f$ and $\Delta J = 0$, then Eq. (2) becomes as

$$\rho_{t_z}(r) \equiv \left\langle J_i \left\| \hat{\rho}^L_{\Delta J=0,t_z}(\vec{r}) \right\| J_i \right\rangle = \frac{1}{\sqrt{4\pi(2J_i+1)}} \sum_{ab} OBDM(J_i, J_i, 0, a, b, t_z) \left\langle j_a \| Y_0 \| j_b \right\rangle R_{n_a l_a}(r) R_{n_b l_b}(r), \quad (6)$$

where

$$\left\langle j_a \| Y_0 \| j_b \right\rangle = \left\langle j_a \left\| \frac{1}{\sqrt{4\pi}} \right\| j_b \right\rangle = \frac{1}{\sqrt{4\pi}} \left\langle j_a \| 1 \| j_b \right\rangle = \frac{1}{\sqrt{4\pi}} \sqrt{2j_a+1}\, \delta_{j_a j_b}. \quad (7)$$

The average occupation number in each orbit n_{a,t_z} is given by

$$n_{a,t_z} = \sqrt{\frac{2J_a+1}{2J_i+1}}\, OBDM(J_i, J_i, 0, a, a, t_z). \quad (8)$$

Exotic nuclei are considered as composite projectiles of mass A_p and described, in Figure-1, as core and valence clusters, of masses A_c and A_v bounded with a state of relative motion. It is assumed that $A_c \geq A_v$. The internal densities of clusters are described by harmonic oscillator wave functions with ranges α_c and α_v.

$$\rho_{t_z c}(r) = \frac{1}{\sqrt{4\pi}} \sqrt{\frac{1}{2J_i+1}} \sum_a OBDM(J_i, a, J=0, t_z, core) \sqrt{2j_a+1}\, \left| R_{n_a l_a}(r) \right|^2 \quad (9)$$

$$\rho_{t_z v}(r) = \frac{1}{\sqrt{4\pi}} \sqrt{\frac{1}{2J_i+1}} \sum_a OBDM(J_i, a, J=0, t_z, valence) \sqrt{2j_a+1}\, \left| R_{n_a l_a}(r) \right|^2 \quad (10)$$

Upon convoluting the intrinsic cluster densities with their center of mass (c.m.) motions about the c.m. of the projectile, the composite projectile density is given by [11]

$$\rho_{t_z,m}(r) = \rho_{t_z,c}(r) + \rho_{t_z,v}(r) \quad (11)$$

For simplicity, the subscript t_z in these densities will be dropped, i.e.

$$\rho_m(r) = \rho_c(r) + \rho_v(r), \quad (12)$$

where $\rho_c(r)$ and $\rho_v(r)$ are given by eq (6) with range parameters

$$\hat{\alpha}_v^2 = \alpha_v^2 + \left(\frac{A_c \alpha}{A_v + A_c} \right)^2, \quad \hat{\alpha}_c^2 = \alpha_c^2 + \left(\frac{A_v \alpha}{A_v + A_c} \right)^2. \quad (13)$$

Furthermore, the matter density of Eq. (12) may also be expressed as

$$\rho_m(r) = \rho^p(r) + \rho^n(r), \quad (14)$$

where $\rho^p(r)$ and $\rho^n(r)$ are the ground state proton and neutron densities of halo nuclei expressed as

$$\rho^p(r) = \rho_c^p(r) + \rho_v^p(r) \quad (15)$$

and

$$\rho^n(r) = \rho_c^n(r) + \rho_v^n(r). \quad (16)$$

The normalization conditions for the ground state densities given in Eqs. (12, 14-16) are

$$g = 4\pi \int_0^\infty \rho_g(r) r^2 dr, \tag{17}$$

and the corresponding rms radii are

$$< r^2 >_g^{1/2} = \frac{4\pi}{g} \int_0^\infty \rho_g(r) r^4 dr, \tag{18}$$

where $\rho_g(r)$ corresponds to the one of the densities [$\rho_m(r)$, $\rho_c(r)$, $\rho_v(r)$, $\rho^p(r)$, $\rho^n(r)$] and g corresponds to the number of nucleons in each case.

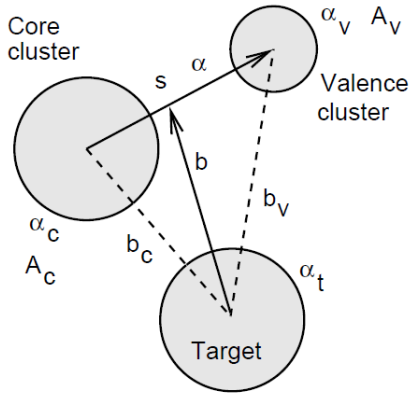

Figure 1- The two-cluster projectile and target coordinates.

The mean squared radius of the composite projectile $< r^2 >_P$ satisfies [11]

$$A_P < r^2 >_P = A_c < r^2 >_c + A_v < r^2 >_v + \frac{A_v A_c}{A_P} < r^2 >= \frac{3}{2}\left(A_v \hat{\alpha}_v^2 + A_c \hat{\alpha}_c^2\right) \tag{19}$$

This approach provides a projectile density with distinct components due to the valence and core clusters. Such simple two component forms can be employed for calculating the density distributions of light exotic nuclei and also employed as input to optical limit calculations of reaction cross sections. However, a particular projectile single particle density, described by a given (A_c,A_v) mass split and choice of the two component ranges ($\hat{\alpha}_c$,$\hat{\alpha}_v$), does not define the underling structure of the projectile. If one of the original clusters is point like, for example $\alpha_v = 0$, then fixing $\hat{\alpha}_v$ and $\hat{\alpha}_c$ uniquely determines α and hence α_c.

Next we use the plane wave Born approximation (PWBA) to study the elastic electron scattering form factors from considered nuclei. In the PWBA, the incident and scattered electron waves are represented by plane waves. The elastic proton form factor is simply given by the Fourier-Bessel transform of the ground state proton density distribution, i.e.

$$F(q) = \frac{4\pi}{Z} \int_0^\infty \rho^p(r) j_0(qr) r^2 dr, \tag{20}$$

where $j_0(qr)$ is the spherical Bessel function of order zero and q is the momentum transfer from the incident electron to the target nucleus. Inclusion of the corrections of the finite nucleon size

$F_{fs}(q) = \exp(-0.43q^2/4)$ and the center of mass $F_{cm}(q) = \exp(b^2q^2/4A)$ in the calculations needs multiplying the form factor of Eq. (20) by these corrections.

In this study, the quadrupole form factor $F_{C2}(q)$, which is important in ^{7}Li and ^{9}Be nuclei, is described by the undeformed p-shell model as [12] :

$$F_{C2}(q) = \frac{\langle r^2 \rangle}{Q}\left(\frac{4}{5P_J}\right)^{1/2} \int j_2(qr)\rho_2^p(r)r^2 dr \quad (21)$$

where $j_2(qr)$ is the second order of the spherical Bessel functions, Q is the quadrupole moment and considered as a free parameter to fit the theoretical form factors with the experimental data and $\rho_2^p(r)$ is the quadrupole proton density distribution assumed, according to the undeformed p-shell model, to be the same as that of ground state proton density distribution $\rho^p(r)$. Then, eq. (21) can be written as [12]:

$$F_{C2}(q) = \frac{\langle r^2 \rangle}{Q}\left(\frac{4}{5P_J}\right)^{1/2} \int j_2(qr)\rho^p(r)r^2 dr \quad (22)$$

Here, P_J is a quadrupole projection factor given as:

$$P_J = J(2J-1)/(J+1)(2J+3) \quad (23)$$

where J is the angular momentum of the ground state.

The reaction cross sections for considered exotic nuclei are studied by the Glauber model [11], where the internal motions of particles within the projectile (P) and target (T) are assumed slow compared to the relative motion of centers of mass of the projectile and target. The reaction cross section for a projectile incident upon a target is given by [13]

$$\sigma_R = 2\pi\int_0^\infty b[1-T(b)]db\left(1-\frac{B_c}{E_{cm}}\right), \quad (24)$$

where B_c is Coulomb barrier, E_{cm} is the kinetic energy in the center of mass system and $T(b)$ is the transparency function at impact parameter b. A straightforward calculation of $T(b)$ is very complicated. One of the simplest methods to calculate $T(b)$ is the optical limit (OL) approximation. In this approximation, which ignores any correlations between particles in the projectile or target, $T(b)$ is written as the squared modulus of the elastic $S-$matrix for the projectile-target system [14]

$$T(b) = \left|S_{el}^{OL}(b)\right|^2, \quad (25)$$

where

$$S_{el}^{OL}(b) = \exp\left[i\mathrm{O}_{PT}(b)\right], \quad (26)$$

and

$$\mathrm{O}_{PT}(b) = \int_{-\infty}^{\infty} dR_3 \int d\vec{r}_1 \int d\vec{r}_2 \rho_P(r_1)\rho_T(r_2) f_{NN}\left(\left|\vec{R}+\vec{r}_1-\vec{r}_2\right|\right) \quad (27)$$

is the overlap of the projectile and target ground state densities (ρ_P and ρ_T, respectively) with an effective nucleon-nucleon (NN) amplitude [$f_{NN}(r)$] integrated along the assumed straight line path of the projectile's center of mass at impact parameter b. For zero-range NN amplitude and isospin $T=0$ target, $f_{NN}(r)$ has the form [14]

$$f_{NN}(r) = (i\bar{\sigma}_{NN}/2)\delta(r) \quad (28)$$

where $\overline{\sigma}_{NN}$ is the average of the free neutron-neutron (nn) and neutron-proton (np) total cross section at the energy of interest. An explicit form for $\overline{\sigma}_{NN}$ is given in ref. [15].

Expressing the projectile-target separation in cylindrical coordinates $\vec{R} = (\vec{b}, R_3)$, where $z = 3$ is the axis chosen along the incident beam direction, then [with the help of Eqs. (27) and (28)] Eq. (26) gives

$$S_{el}^{OL}(b) = \exp\left[-\frac{\overline{\sigma}_{NN}}{2} \int d\vec{r}_1 \int d\vec{r}_2 \rho_P^z(r_1) \rho_T^z(r_2) \delta(\left|\vec{b} + \vec{r}_1 - \vec{r}_2\right|) \right]. \quad (29)$$

Integrating over the coordinates r_2 then replacing r_1 by s, we obtain

$$S_{el}^{OL}(b) = \exp\left[-\frac{\overline{\sigma}_{NN}}{2} \int d\vec{s} \rho_P^z(s) \rho_T^z(\left|\vec{b} + \vec{s}\right|) \right], \quad (30)$$

where $\rho_{P(T)}^z(s)$ is the z-direction integrated nucleon density distribution expressed as

$$\rho_{P(T)}^z(s) = \int_{-\infty}^{\infty} \rho_{P(T)}\left(\sqrt{s^2 + z^2}\right) dz. \quad (31)$$

with *s* the projection of *r* in the impact parameter plane.

It is obvious from Eq. (30) that the calculations of $S_{el}^{OL}(b)$ requires only the projectile and target ground state densities. For simplicity, both densities are described by single Gaussian functions with range parameters α_P and α_T, respectively.

Results and discussion

The ground state proton, neutron and matter densities of the ^{11}Li ($S_{2n} = 0.3$ MeV, $\tau_{1/2} = 8.8$ ms) [16, 17] and ^{12}Be ($S_{2n} = 3.67$ MeV, $\tau_{1/2} = 20$ ms) [16, 17] exotic nuclei are studied by means of the BCM [11]. The exotic nucleus is considered as a composite projectile consisting of core and valence clusters bound with a state of relative motion [Figure-1]. The internal densities of the clusters, given by Eqs. (9) and (10), are described by single particle harmonic oscillator wave functions. The composite projectile densities of ^{11}Li and ^{12}Be are calculated by Eq. (12). The nucleus ^{11}Li ($J^\pi, T = 3/2^-, 5/2$) is formed by coupling the core ^{9}Li ($J^\pi, T = 3/2^-, 3/2$) with the valence two neutrons ($J^\pi, T = 0^+, 1$). The nucleus ^{12}Be ($J^\pi, T = 0^+, 2$) is formed by coupling the core ^{10}Be ($J^\pi, T = 0^+, 1$) with the valence two neutrons ($J^\pi, T = 0^+, 1$). The configurations $(1s_{1/2})^4$, $(1p_{3/2})^5$ and $(1s_{1/2})^4$, $(1p_{3/2})^6$, are assumed for core nuclei ^{9}Li and ^{10}Be, respectively. Four different configurations are considered for the description of the two valence neutrons in ^{11}Li and ^{12}Be. The two valence neutrons are assumed to be in the pure $1p_{1/2}$, the pure $1d_{5/2}$, the pure $2s_{1/2}$ and the model space of Zuker-Buck- Mcgrory (ZBM), which includes the orbitals, $1p_{1/2}$, $1d_{5/2}$ and $2s_{1/2}$.

To obtain the OBDM elements for the two valence neutrons occupying the model space ZBM, shell model calculations are performed via the computer code OXBASH [10] using the realistic interaction of REWIL [18]. The ground state occupation numbers for the two valence neutrons in ^{11}Li and ^{12}Be are 1.605 for $(1p_{1/2})^2$, 0.345 for $(1d_{5/2})^2$ and 0.050 for $(2s_{1/2})^2$. These occupation numbers indicate that the structures of the two valence neutrons in ^{11}Li and ^{12}Be is mixed configurations with dominant $(1p_{1/2})^2$. As the halo nucleons prefer to occupy orbits with low orbital quantum numbers (such as the s or p-orbital), these occupation numbers supports the halo structure of these nuclei.

Figure- 2 shows the dependence of the matter density distributions (in fm^{-3}) on r (in fm) for ^{11}Li Figure- 2(a) and ^{12}Be Figure- 2(b) exotic nuclei. The long-dashed, dashed, dash- dotted and solid lines are the calculated results when the valence two neutrons in ^{11}Li and ^{12}Be move in the pure $1p_{1/2}$ orbit, the pure $1d_{5/2}$ orbit, the pure $2s_{1/2}$ orbit and the model space of ZBM, respectively. The experimental matter densities (denoted by the shaded area) of ^{11}Li [19] and ^{12}Be [20] are also displayed for comparison. It is

clear from Fig. 2 that the performance of the long-dashed and solid distributions are approximately the same throughout the entire range of considered r. In addition, the long-dashed and solid distributions are better describing the data than the others.

Figure- 3 demonstrates the contributions of the core nucleons (dashed lines) and the two valence neutrons (dash- dotted lines) to the matter density (solid lines) for exotic nuclei ^{11}Li Figure- 3(a) and ^{12}Be Figure- 3(b). The feature of the long tail behavior (considered as a distinctive feature of halo nuclei) is exemplified in the solid distributions of Figure- 3. Hence, this behavior (which is due to the two valence neutrons) is in agreement with the experimental data.

Figure- 4 illustrates the calculated proton and neutron density distributions displayed as dashed and dash- dotted lines, respectively. The long tail performance is clearly noticed in the dash- dotted lines. This performance is related to the existence of the valence two neutrons in the halo orbits. The steep slope performance is obviously observed in the dashed lines due to the absence of protons in the halo orbit, where all protons of these nuclei are found in their cores only.

To seek out if the long tail behavior of the matter density distribution of the neutron rich nuclei demonstrates noticeable effects in the process of elastic electron scattering, elastic charge form factors for unstable neutron rich ^{11}Li (^{12}Be) and its stable ^{7}Li (^{9}Be) are calculated by means of the Plane Wave Born Approximation (PWBA). To compare the results of the form factor of the unstable nucleus ^{11}Li (^{12}Be) with that of the stable nucleus ^{7}Li (^{9}Be), first present the calculated proton (C_0+C_2) form factors of ^{7}Li (^{9}Be) compared with the measured data taken from reference [21] ([22]). The calculated form factors in Figures- 5 (a) and 5 (b) correspond to ^{7}Li and ^{9}Be nuclei, respectively. The experimental data are very well reproduced by our calculations. The C_0 and C_2 contributions are shown in this figure by the dashed and dash- dotted lines, respectively.

Figure- 6 exemplifies the comparison between the calculated elastic C_0 proton form factors of the unstable nuclei ^{11}Li and ^{12}Be (dashed lines) and those of the stable nuclei ^{7}Li and ^{9}Be (solid lines). Figs. 6(a) and 6(b) demonstrate the proton form factors for nuclei pairs (^{11}Li, ^{7}Li) and (^{12}Be, ^{9}Be), respectively. It is well known that the proton form factor is independent of the detailed properties of the two valence neutrons. The major difference between the calculated form factors of the unstable nuclei (^{11}Li and ^{12}Be) and those of the stable nuclei (^{7}Li and ^{9}Be) is the difference in the center of mass correction, which depends on the mass number and the size parameter α, which is assumed in this case equal to the average of α_c and α_v. It is clearly noticed that the dashed and solid lines in Fig. 6 have only one diffraction minimum and one diffraction maximum.

The reaction cross sections (σ_R) are studied by means of the Glauber model with an optical limit approximation at high energies for (^{11}Li and ^{12}Be) projectiles incident on the ^{12}C target using the ground state densities of these nuclei. The densities of projectile and target are described by single Gaussian functions with range parameters α_P and α_T for projectile and target nuclei, respectively [11]. The calculated reaction cross sections are listed in Table (1) along with the corresponding experimental data taken from refs. [23,24]. The calculated σ_R at 790 MeV for ^{11}Li + ^{12}C system is 1064 mb, which agrees with the analogous measured data 1060 ± 10 mb within the quoted error [23]. The calculated σ_R at 790 MeV for ^{12}Be + ^{12}C system is 937 mb, which agrees with the corresponding experimental data 927 ± 18 mb within the quoted error [24].

Table 1- Calculated reaction cross sections for ^{11}Li and ^{12}Be exotic nuclei.

Exotic Nucleus	Experimental rms radii (fm)	Calculated σ_R (mb)	Experimental σ_R (mb)	Energy (MeV) [23, 24]
^{11}Li	3.27 ± 0.24 [23]	1064	1060 ± 10 [23]	790
^{12}Be	2.55 ± 0.09 [20]	937	927 ± 18 [24]	790

Conclusions

The ground state proton, neutron and matter density distributions of unstable neutron- rich ^{11}Li and ^{12}Be exotic nuclei are investigated using the binary cluster model (BCM). Elastic electron scattering from these two exotic nuclei are also investigated. The long tail behavior, considered as a distinctive feature of halo nuclei, is evidently revealed in the calculated neutron and matter density distributions of these two exotic nuclei. Besides, the noticeable difference that is found between the calculated overall proton and neutron rms radii also indicates a definite degree of halo structure. It is found that the difference between the form factors of unstable exotic nucleus ^{11}Li [^{12}Be] and that of a stable nucleus ^{7}Li [^{9}Be] is the difference in the center of mass correction which depends on the mass number and the size parameter α. The calculated reaction cross sections of ^{11}Li and ^{12}Be at high energy (790 MeV) are in agreement with those of experimental data. The analysis of the present study suggests that the structure of the two valence neutrons in ^{11}Li [^{12}Be] is mixed configurations with dominant $(1p_{1/2})^2$. The present study supports the halo structure of these nuclei.

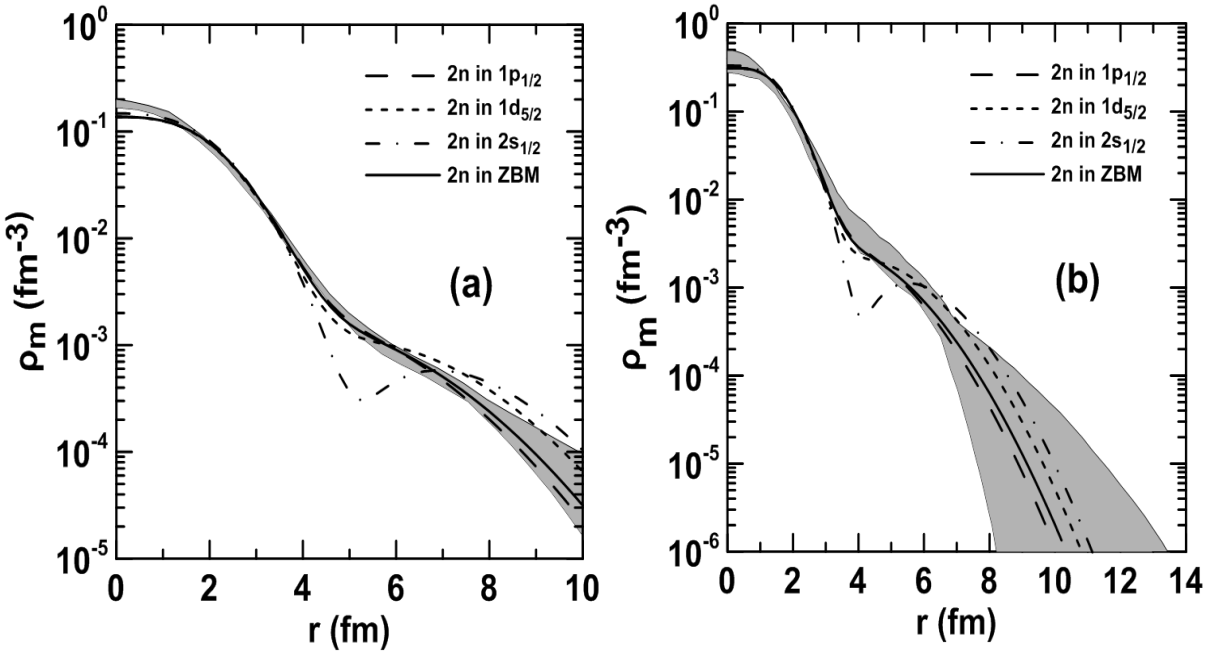

Figure 2- The calculated matter density distributions for exotic nuclei ^{11}Li [(a)] and ^{12}Be [(b)]. The shaded area are the experimental data of ^{11}Li [19] and ^{12}Be [20].

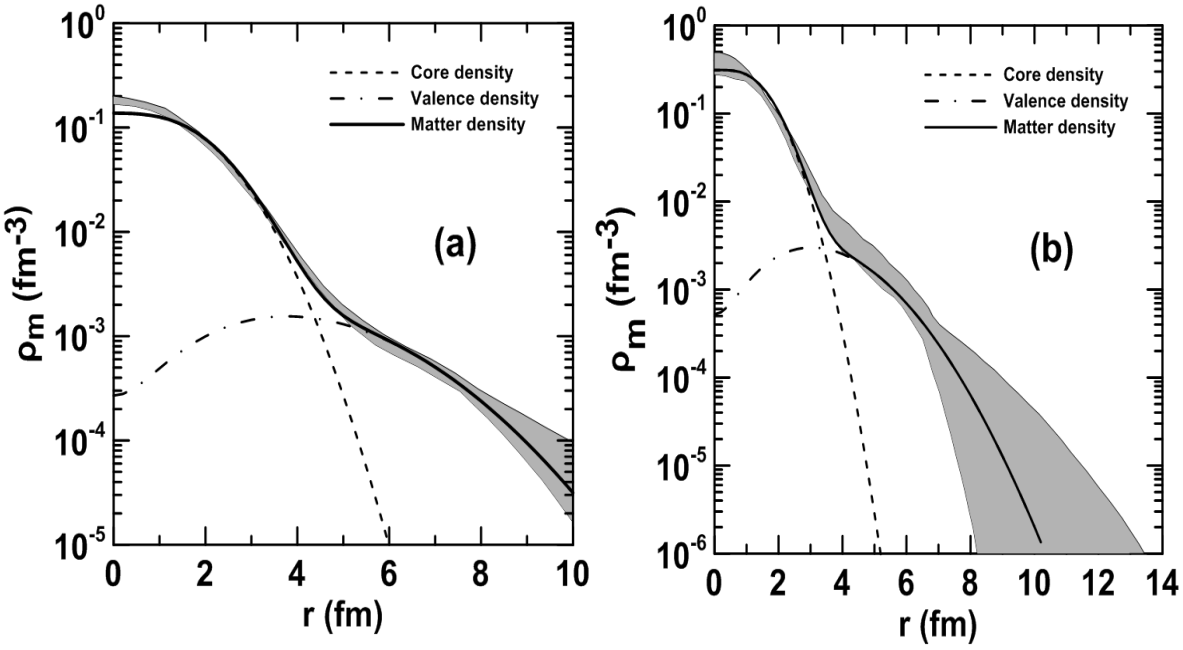

Figure 3-The calculated matter density distributions for exotic nuclei ^{11}Li [(a)] and ^{12}Be [(b)]. The shaded area are the experimental data of ^{11}Li [19] and ^{12}Be [20].

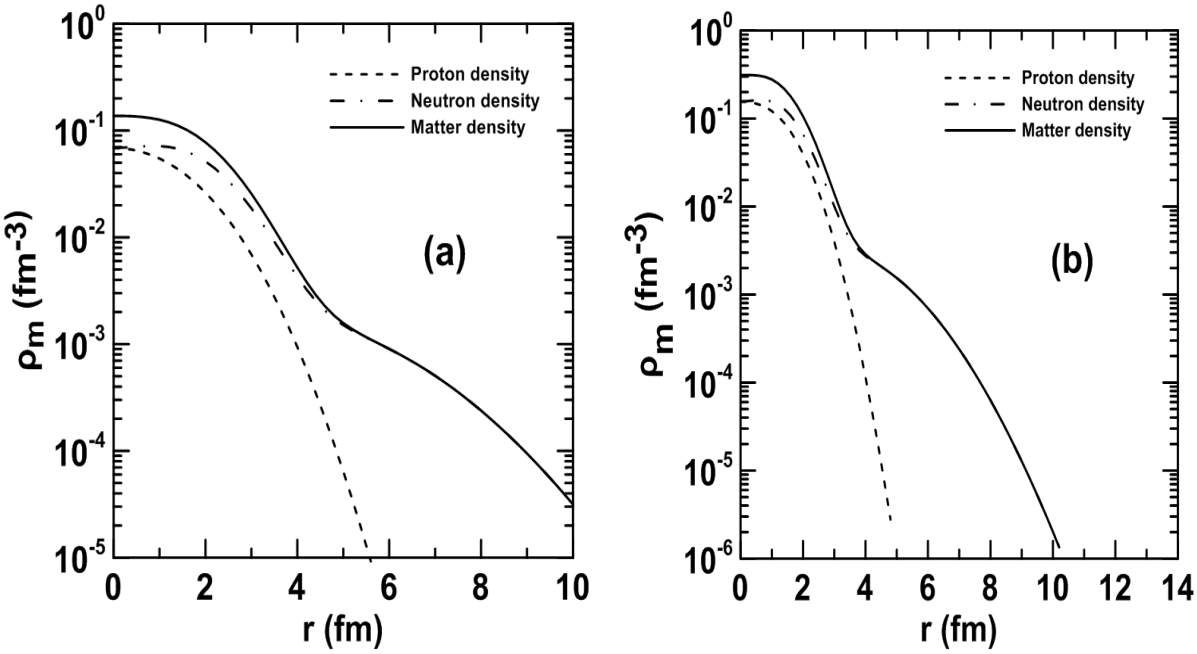

Figure 4- Neutron, proton and matter density distributions for exotic nuclei ^{11}Li [(a)] and ^{12}Be [(b)].

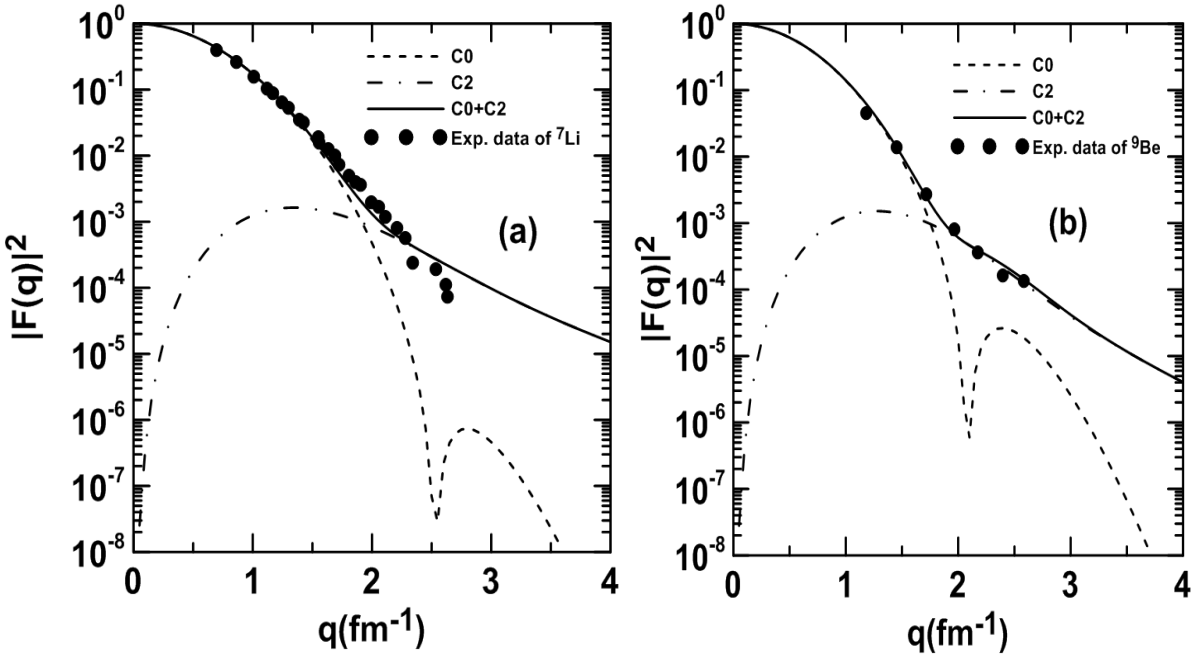

Figure 5- Proton form factors of stable nuclei ^{7}Li and ^{9}Be. The experimental data of ^{7}Li and ^{9}Be are taken from ref. [21] and [22], respectively.

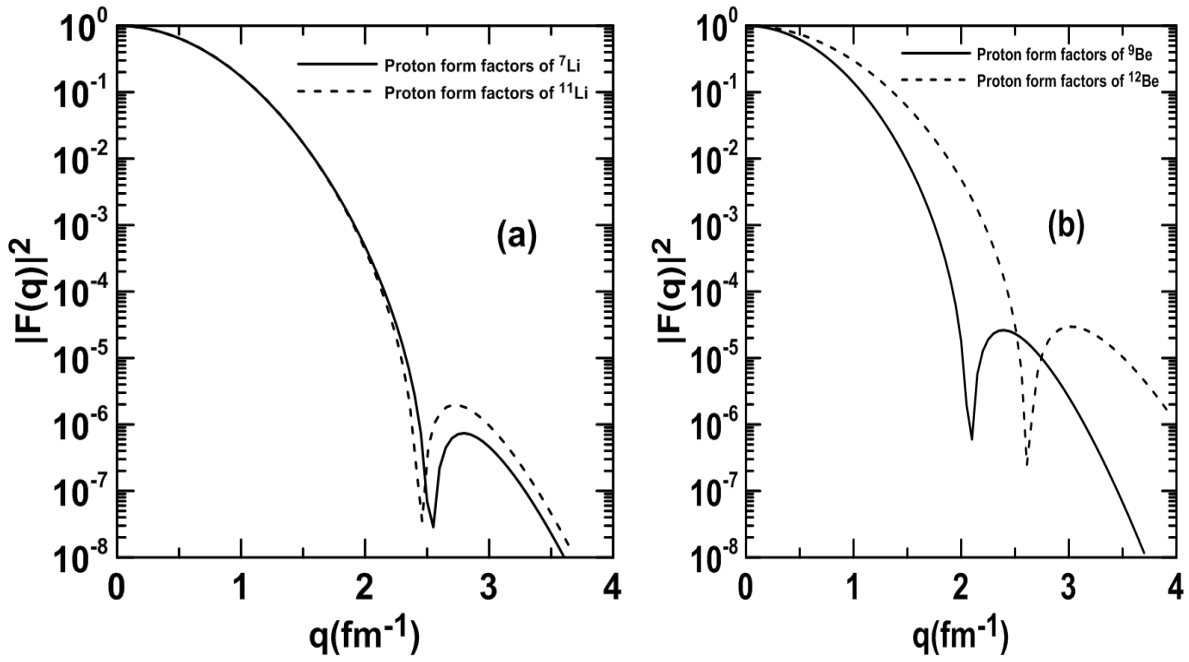

Figure 6- Comparison between the calculated proton form factors of unstable (exotic) nuclei (^{11}Li, ^{12}Be) and those of stable nuclei (^{7}Li, ^{9}Be).

References

1- Tanihata I. **1996**. Neutron halo nuclei. *J. Phys*. G **22**, pp: 157-198.

2- Donnelly T.W. and Sick I. **1984**. Elastic magnetic electron scattering from nuclei. *Reviews of Modern Physics*, 56, 461-566.

3- Wapstra A. H., Audi G., and Hoekstra R. **1988**. Atomic masses from (mainly) experimental data. *Atomic Data and Nuclear Data Tables*, 39, pp: 281-287.

4- I. Tanihata. **1995**. Nuclear structure studies from reaction induced by radioactive nuclear beams. *Prog. Part. Nucl. Phys*. **35**, pp: 505-573.

5- Zhang H.Y., Shen W.Q., Ren Z.Z., Ma Y.G., Jiang W.Z., Zhu Z.Y., Cai X.Z., Fang D.Q., Zhong C., Yu L.P., Wei Y.B., Zhan W.L., Guo Z.Y., Xiao G.Q., Wang J.S., Wang J.C., Wang Q.J., Li J.X., Wang M. and Chen Z.Q.**2002**. Measurement of reaction cross section for proton-rich nuclei (A<30) at intermediate energies. *Nuclear Physics* A 707, pp: 303–324.

6- Tel E., Okuducu S., Tamr G., Akti N.N. and Bolukdemir M. II. **2008.** Calculation of radii and density of $^{7-19}$b isotopes using effective skyrme force. *Commun. Theor. Phys.* 49, pp: 696–702.

7- Hamoudi A. K., Flaiyh G. N. and Abdullah A. N. **2015**.Study of Density Distributions, Elastic Electron Scattering form factors and reaction cross sections of ^{9}C, ^{12}N and ^{23}Al exotic nuclei, *Iraqi Journal of Science*, 56 (1A): 147-161.

8- Jun G.W., Qing J. H., Ye L. J., Wei Z., Zhou R. Z., and Guo L. X. **2003**. Total nuclear reaction cross section induced by halo nuclei and stable nuclei. *Commun. Theor. Phys*. **40,** pp: 577–584.

9- Brown B. A., Radhi R. and Wildenthal B. H. **1983**. Electric quadrupole and hexadecupole nuclear excitations from the perspectives of electron scattering and modern shell-model theory. *Physics Reports*. **101**(5),pp: 313-358.

10- Brown B. A., Etchegoyen A., Godwin N. S.,Rae W. D. M., Richter W. A., Ormand W.E., Warburton E. K., Winfield J. S., Zhao L., Zimmerman C. H. 2005. Oxbash for Windows PC. MSU-NSCL report number 1289.

11- Tostevin J. A., Johnson R. C. and Al-Khalili J. S.**1998**. Manifestation of halo size in scattering and reactions. *Nuclear Physics* A **630**, pp: 340c-351c.

12- Stovall T., Goldemberg J. and Isabelle D. B.**1966**. Coulomb form factors of ^{10}B and ^{11}B. *Nuclear Physics*, **86,** pp: 225-240.

13- Zheng T., Yamaguchi T., Ozawa A., Chiba M., Kanungo R., Kato T., Katori K., Morimoto K., Ohnishi T., Suda T., Tanihata I., Yamaguchi Y., Yoshida A., Yoshida K., Toki H. and Nakajima N. **2002**. Study of halo structure of ^{16}C from reaction cross section measurement. *Nuclear Physics* A **709**, pp: 103-118.

14- Tostevin J. A. and Al-Khalili J. S. **1997**. How large are the halos of light nuclei. *Nuclear Physics* A **616** , pp: 418c-425c.

15- Charagi S.K. and Gupta S.K. **1990**. Coulomb-modified Glauber model description of heavy-ion reaction cross sections. *Physical Review* C **41**, pp: 1610-1618.

16- Audi G, Wapstra A. H. and Thibault C. **2003**. The AME 2003 atomic mass evaluation (II). Tables, graphs and references. *Nuclear Physics* A 729, pp: 337–676.

17- Audi G., Bersillon O., Blachot J. and Wapstra A.H. **2003.** The NUBASE evaluation of nuclear and decay properties. *Nuclear Physics* **A** 729, pp: 3-128

18- McGrory J. B. and Wildenthal B. H. **1973**. Shell-model calculations for A=18,19, and 20 nuclei with core excitation included explicity. *Physical Review* C **7**, 974.

19- Antonov A. N., Kadrev D. N., Gaidarov M. K., Moya de Guerra E., Sarriguren P., Udias J. M., Lukyanov V. K., Zemlyanaya E. V., and Krumova G. Z. **2005**. Charge and matter distributions and form factors of light, medium, and heavy neutron-rich nuclei. *Physical Review* C **72**, pp: 1-11.

20- Ilieva S. **2008**. Investigation of the nuclear matter density distribution of the exotic ^{12}Be, ^{14}Be and ^{8}Bnuclei by elastic proton scattering in inverse kinematics. Ph.D. Thesis, der Johannes Gutenberg University, Mainz.

21- Suelzle L. R., Yearian M. R. and Crannell H. **1967**. Elastic electron scattering from ^{6}Li and ^{7}Li. *Physical Review* 162, p.992.

22- Bernheim M., Stovall T. and Vinciguerra D. **1967**. Electron scattering from ^{9}Be. *Nuclear Physics* A 97, p.488 .

23- Tanihata I., Hamagaki H., Hashimoto O., Shida Y., Yoshikawa N., Sugimoto K., Yamakawa O, and Kobayashi T.**1985**. Measurement of interaction cross sections and nuclear radii in the light p-shell region. *Physical Review Letters*, **55** (24), pp: 2676-2679.

24- Ozawa A., Suzuki T. and Tanihata I.**2001**. Nuclear size and related topics. *Nuclear Physics* A 693,pp: 32–62.